International Journal of Psychophysiology 94 (2014) 482–495

Contents lists available at ScienceDirect

International Journal of Psychophysiology

journal homepage: www.elsevier.com/locate/ijpsycho

Optimal set of EEG features for emotional state classification and trajectory visualization in Parkinson's disease

R. Yuvaraj [a,*], M. Murugappan [a], Norlinah Mohamed Ibrahim [b], Kenneth Sundaraj [a], Mohd Iqbal Omar [a], Khairiyah Mohamad [b], R. Palaniappan [c]

[a] School of Mechatronic Engineering, University Malaysia Perlis (UniMAP), Campus Ulu Pauh, Arau, 02600, Perlis, Malaysia
[b] Neurology Unit, Department of Medicine, UKM Medical Center, Jalan Yaacob Latiff, 56000, Bandar Tun Razak, Kuala Lumpur, Malaysia
[c] School of Computing, University of Kent, Medway, UK

ARTICLE INFO

Article history:
Received 14 May 2014
Received in revised form 24 July 2014
Accepted 31 July 2014
Available online 7 August 2014

Keywords:
Electroencephalogram
Emotion classification
Feature reduction
Manifold learning
Parkinson's disease

ABSTRACT

In addition to classic motor signs and symptoms, individuals with Parkinson's disease (PD) are characterized by emotional deficits. Ongoing brain activity can be recorded by electroencephalograph (EEG) to discover the links between emotional states and brain activity. This study utilized machine-learning algorithms to categorize emotional states in PD patients compared with healthy controls (HC) using EEG. Twenty non-demented PD patients and 20 healthy age-, gender-, and education level-matched controls viewed happiness, sadness, fear, anger, surprise, and disgust emotional stimuli while fourteen-channel EEG was being recorded. Multimodal stimulus (combination of audio and visual) was used to evoke the emotions. To classify the EEG-based emotional states and visualize the changes of emotional states over time, this paper compares four kinds of EEG features for emotional state classification and proposes an approach to track the trajectory of emotion changes with manifold learning. From the experimental results using our EEG data set, we found that (a) bispectrum feature is superior to other three kinds of features, namely power spectrum, wavelet packet and nonlinear dynamical analysis; (b) higher frequency bands (alpha, beta and gamma) play a more important role in emotion activities than lower frequency bands (delta and theta) in both groups and; (c) the trajectory of emotion changes can be visualized by reducing subject-independent features with manifold learning. This provides a promising way of implementing visualization of patient's emotional state in real time and leads to a practical system for noninvasive assessment of the emotional impairments associated with neurological disorders.

1 . Introduction

Parkinson's disease (PD) is a neurodegenerative disorder associated with the loss of dopamine-producing neurons in the basal ganglia. The cardinal symptoms of the disease are tremor, muscular rigidity, bradykinesia (i.e., slowness of movement), and postural instability. These motor impairments are often accompanied by a wide range of non-motor symptoms (e.g., depression, executive dysfunctions, sleep disturbances, autonomic impairments), both symptom categories having a great impact on the quality of PD patient's life (Martinez-Martin et al., 2011).

Over the last decade, there has been an increasing attention to the role played by emotional processes in PD (Gray and Tickle-Degnen, 2010; Péron et al., 2012). Evidence indicates the individuals with PD have deficits in recognizing emotions from prosody (Dara et al., 2008; Pell and Leonard, 2003; Yip et al., 2003) and facial expressions (Ariatti et al., 2008; Clark et al., 2008; Dujardin et al., 2004), although not all findings have been consistent. Several studies have failed to find impaired performance in the recognition of facial expressions related to emotion in their PD samples (Adolphs et al., 1998; Pell and Leonard, 2005), whereas others have failed to find deficits in recognition from prosody (Clark et al., 2008; Kan et al., 2002). In a recent meta-analysis of the literature comparing emotional recognition abilities of individuals with PD and healthy controls (HC), Gray and Tickle-Degnen concluded that there is a robust link between PD and deficits in emotion recognition using both voice and faces, with impairments particularly marked with respect to negative emotions (Gray and Tickle-Degnen, 2010). A commonly drawn inference is that the emotion recognition deficit experienced by individuals with PD is likely to be cross-modal (Peron et al., 2010), yet only a small number of studies have examined emotion recognition performance in both facial and prosodic modalities with same participants. A number of these reports found deficits in both modalities (Ariatti et al., 2008; Yip et al., 2003), whereas others found

* Corresponding author at: School of Mechatronic Engineering, University Malaysia Perlis (UniMAP), Campus Ulu Pauh, Arau, Perlis 02600, Malaysia. Tel.: +60 14 6011990; fax: +60 4 988 5167.
E-mail address: yuva2257@gmail.com (R. Yuvaraj).

http://dx.doi.org/10.1016/j.ijpsycho.2014.07.014
0167-8760/

problems in only one modality (facial, Pell and Leonard, 2003); prosody, Pell and Leonard, 2005), and at least one failed to find deficits in recognition in either modality (Caekebeke et al., 1991).

Furthermore, there is sparse event related potential (ERP) evidence that early processing of emotional prosody (mismatch negativity, Schröder et al., 2006) and faces (early posterior negativity, Wieser et al., 2012) may be affected in PD. Altogether, experimental evidence does support the view of deficits in emotion processing in PD patients. However, much of the research in this area focused on the patient's behavioral responses (i.e. participants were asked to match, identify or rate the emotional stimuli) and few studies have measured physiological response to emotions (e.g., ERPs). The existing literature mentioned above used traditional statistical analysis tools for the investigation of emotion processing in PD. There is little quantitative objective measurement that correlates with the emotional impairment in neurological disorder patients compared to healthy control participants. This underlines the need for an objective quantitative measure of emotional processing that can identify and compute subtle changes in emotional states and hence help in a group based comparative analysis between PD patients and HC, thereby enabling the assessment of emotional impairment treatment efficacy and progression of the disease.

Numerous studies on engineering approaches to automatic emotion recognition have been performed with healthy participants in the past few decades. They can be categorized into three main approaches. The first kind of approach focuses on the analysis of facial expressions, speech, or gesture (Anderson and McOwan, 2006; Gunes and Piccardi, 2007; Kessous et al., 2010). These audio-visual based techniques allow noncontact detection of emotions, so they do not give any discomfort to the subject. However, these techniques might be more prone to deception, and the parameters vary in different situations. The second kind of approach focuses on peripheral physiological signals. Various studies show that peripheral physiological signals varying for different emotional states can be observed through changes of the autonomic nervous system (ANS) in the periphery, such as electrocardiogram (ECG), skin conductance (SC), electromyogram (EMG), respiration rate (RR), and pulse (Valenza et al., 2012). In comparison with audio-visual based methods, the responses of peripheral physiological signals tend to provide more detailed information as indicator for estimating emotional states. The third kind of approach focuses on brain signals captured from the central nervous system (CNS) such as electroencephalogram (EEG), Magnetoencephalogram (MEG), Positron Emission Tomography (PET), and functional Magnetic Resonance Imaging (fMRI). Among these, EEG appears to be less invasive and the one with best time resolution as compared to the other methods (MEG, PET, and fMRI). In addition, EEG signals have been proved to provide informative characteristics in responses to the emotional states (Petrantonakis and Hadjileontiadis, 2011).

Recently, emotion classification using EEG data has attracted much attention with the rapid development of dry electrodes, digital signal processing methods, machine-learning techniques, and various real-world applications of brain computer interface (BCI) for healthy controls. However, there still exist some limitations on traditional EEG-based emotion recognition framework. One of the major limitations is that almost all existing methods do not consider the characteristics of EEG and emotion. In general, EEG is unsteady rapidly changing voltage signal and the features extracted from EEG usually change dramatically, whereas emotions only change gradually. This leads to wider differences among EEG features, even with the same emotional state in adjacent time periods. Moreover, existing studies with HC are only able to predict the labels of emotion samples, but could not reveal the trend of changes in the emotion. To overcome these limitations, in this paper, we introduce an approach to track the trajectory of emotion changes in PD patients compared to HC. In order to validate the effectiveness of the proposed method we compare four kinds of EEG-emotion-specific features, and evaluate the classification performance of six emotional states (happiness, sadness, fear, anger, surprise and disgust) of PD patients in comparison with age-, education level- and gender-matched HC.

The rest of the paper is organized as follows: Section 2 provides an overview of related work on various methods for EEG-based emotion classification in HC. Section 3 presents the participants' characteristics and experiment setting for emotion induction. A description of feature extraction, feature dimensionality reduction, classification, and trajectory of emotion changes is given in Section 4. Finally in Section 5, we present the experimental results that we obtained. Conclusions and future work are presented at the end.

2 . Related work

Since EEG not only indicates emotional states, but also reflects other cognitive activities of the brain. The selection of independent variables to discriminate emotions from the EEG across various electrode locations is not very self-evident, thus recently researchers explored complex methods to find the correlation between the emotional changes and EEG signals. Zhang and Lee reported an average accuracy of 73.00% $\pm$ 0.33% by using EEG features to categorize subject's status into two emotional states (Zhang and Lee, 2009). Chanel et al. obtained an average accuracy of 63% by using EEG time–frequency information as features for three emotional classes (Chanel et al., 2009). Lin et al. (2010) used EEG signals to recognize emotions in response to emotional music. Their study achieved a recognition rate of 82.29% $\pm$ 3.06% for four emotional states (Lin et al., 2010). Murugappan et al. (2010) attained a maximum average accuracy of 83.26% for distinguishing five emotional states using different set of EEG channels (Murugappan et al., 2010). Petrantonakis and Hadjileontiadis (2010) proposed a user-independent emotion-estimation system for recognizing six emotional states; with the average accuracy of 83.33% achieved (Petrantonakis and Hadjileontiadis, 2010). Moreover, evidence of brain activity relating to affective responses is reported in the majority of EEG frequency bands, i.e., *theta* (4–8 Hz), *alpha* (8–13 Hz), *beta* (13–30 Hz), and *gamma* (30–49 Hz) (Aftanas et al., 2004; Davidson, 2004). Frontal midline (Fm) *theta* power modulation is suggested to reflect affective processing during emotional stimuli (Sammler et al., 2007). The *alpha*-power asymmetry on the prefrontal cortex has been proposed as an index for the discrimination between positively and negatively valenced emotions (Davidson, 2004; Schmidt and Trainor, 2001). *Beta* activity has been associated with emotional arousal modulation (Aftanas et al., 2006) and also, asymmetric activity in this band is linked to the emotional dimensions of approach or withdrawal (Schutter et al., 2001). Finally, *gamma* band has been mainly suggested as related to arousal effects (Balconi and Lucchiari, 2008).

3 . Materials

3.1 . Recruitment of eligible participants

Twenty non-demented PD patients (10 men and 10 women) and 20 healthy controls (9 men and 11 women) matched for age (range from 40 to 65 years), education level, and gender participated in the study. The PD patients were recruited through the Neurology Unit outpatient service at the Department of Medicine of the Hospital University Kebangsaan Malaysia (HUKM) medical center in Kuala Lumpur, Malaysia. All of them had been diagnosed with Idiopathic PD by a neurologist. Patients who had coexisting neurological disturbances (e.g., epilepsy, stroke) or who had undergone deep brain stimulation were not included in the study. The HC participants were recruited through the hospital community and/or from relatives of PD patients.

Exclusion criteria for controls included any current psychiatric or neurological disorder. Exclusion criteria for both groups were dementia or depression as indicated by a score of 24 or lower on the mini mental state examination (MMSE) (Folstein et al., 1975; Wieser et al., 2012) or 18 or higher on the Beck Depression Inventory (BDI) (Beck et al., 1961;

Schröder et al., 2006). All participants were right-handed as determined by self-report and confirmed by Edinburgh Handedness Inventory (EHI) (Oldfield, 1971). This test consisted of 10 questions asking for the preferred hand for a series of activities (e.g. writing, throwing, using scissors, etc.). All participants reported normal or corrected-to-normal vision and intact hearing was formally established in all participants by administering a pure tone audiometric screening of both ears to ensure acceptable normal hearing threshold (minimum 30 dB HL at 0.5, 1, 2, and 4 kHz, for the better ear).

3.2 . Participant's characteristics

Demographic and clinical characteristics of patients with PD and healthy controls are presented in Table 1. Patients and controls were comparable in demographic variables such as age (PD: mean age = 59.05 ± 5.64 years; HC: mean age = 58.10 ± 2.95 years), t (38) = 0.667, $p = 0.509$, gender distribution (PD: 10 men, HC: 09 men), $x^2(1, N = 40) = 0.100$, $p = 0.752$, and education level (PD: 10.45 ± 4.86 years; HC: 11.05 ± 3.34 years), t (38) = −0.455, $p = 0.652$. Furthermore, PD patients and HC did not differ in mean MMSE scores, mean BDI scores as well as mean EHI scores.

The severity of motor symptoms corresponded to Stages I–III (Stage I = unilateral disease with mild symptoms, Stage II = bilateral involvement, Stage III = bilateral symptoms with postural and gait disturbances) of the Hoehn and Yahr scale (Hoehn and Yahr, 1967) and to an average score of 17.05 ± 3.15 in the motor scale of the Unified Parkinson's Disease Rating Scale (UPDRS) (Fahn et al., 1987). Motor symptoms were characterized as left dominant (n = 11) and right dominant (n = 9). Duration of the disease varied between 1 and 12 years, with a mean of 5.75 ± 3.52 years. All of the patients were undergoing dopamine replacement therapy and were tested while being administered their anti-Parkinsonian medication (i.e. during their "ON" state), distributed as follows: d2-agonist (n = 18); carbidopa/L-dopa (n = 13), monoamine oxidase B (MAO-B) inhibitor (n = 7), catechol-O-methyltransferase (COMT) inhibitor (n = 5), amantadine (n = 5), or anticholinergics (n = 3).

3.3 . Ethics statement

This study was approved by the ethics committee of the HUKM and written informed consent was obtained according to the Declaration of Helsinki. Participants were financially compensated (50 Malaysian Ringgits) for their time.

Table 1
Demographic and clinical characteristics of patients with PD and healthy controls.

	PD (N = 20)	HC (N = 20)	Test's value	Statistical result*
Age (years)	59.05 ± 5.64	58.10 ± 2.95	$t = 0.667$	$p = 0.509$
Sex	10 F/10 M	11 F/9 M	$x^2 = 0.100$	$p = 0.752$
Education (years)	10.45 ± 4.86	11.05 ± 3.34	$t = -0.455$	$p = 0.652$
MMSE score (0–30)	26.90 ± 1.51	27.15 ± 1.63	$t = -0.502$	$p = 0.619$
Hoehn and Yahr scale (I/II/III)	2.25 ± 0.63	–	–	–
Motor UPDRS score	17.05 ± 3.15	–	–	–
Disease duration (years)	5.75 ± 3.52	–	–	–
BDI score (0–21)	5.80 ± 2.87	5.45 ± 2.18	$t = 0.433$	$p = 0.667$
EHS (1–10)	9.55 ± 0.76	9.84 ± 0.72	$t = -0.818$	$p = 0.403$

Note: N = number of participants, M = male, F = female, MMSE = mini mental state examination, UPDRS = Unified Parkinson's Disease Rating Scale, BDI = Beck Depression Inventory, and EHS = Edinburg Handedness Inventory. Data presented as mean ± SD.
*Difference is significant at the $p < 0.05$ level.

3.4 . Stimulus material

Gathering good and meaningful data is essential in any signal processing application. In works related to emotion recognition using physiological signal, acquiring emotional data that corresponds to specific emotional state is challenging, because of the subjective nature of the emotions and cognitive dependence of physiological signals which requires the emotional states to be elicited internally in the participant. Until now, most studies on emotion recognition in PD have used only facial stimuli, prosodic stimuli, or music stimuli (Gray and Tickle-Degnen, 2010; Lima et al., 2013; Péron et al., 2012). In addition, a number of emotion induction techniques using pictures, sounds, music, or multimodal approach (combination of audio and visual) have been used to elicit the target emotions in healthy controls (Baumgartner et al., 2006; Lin et al., 2010; Murugappan et al., 2010; Petrantonakis and Hadjileontiadis, 2011; Wang et al., 2013). Among all of these stimuli modalities researchers have identified that multimodal stimuli induce emotions in the participants more naturally and more effectively compared to other modalities (Murugappan et al., 2010; Wang and Guan, 2008). In this work, we have utilized a multimodal approach to evoke specific targeted emotional state.

The emotional stimuli we used were taken from different sources such as the International Affective Picture System (IAPS) database (Lang et al., 2008), International Affective Digitized Sounds (IADS) (Bradley and Lang, 2007) database and video clips (e.g., funny animals, wonder activities by humans etc.) collected from various resources on the internet (e.g., YouTube, Facebook, and others) (Murugappan et al., 2010). The elicitation of emotions such as sad, fear, and disgust was attained by using affective pictures from IAPS and sounds from IADS databases. Various psychological and psychophysiological experiments have revealed that these stimuli sets have great potential in the investigation of sad, fear, and disgust emotion [43, 50]. Additionally, Mikels et al. (2005) and Redondo et al. (2008) provided a more complete characterization of the categorical structure of the IAPS and IADS stimuli set, with the objective of identifying images and sounds that elicit one discrete emotion more than other emotions. The IAPS pictures[1] [*disgust*: valence mean ± SD = 2.43 ± 1.51, arousal mean ± SD = 5.90 ± 2.25; *fear*: valence mean ± SD = 3.80 ± 1.89, arousal mean ± SD = 5.85 ± 2.12; *sadness*: valence mean ± SD = 2.74 ± 1.57, arousal mean ± SD = 5.00 ± 2.08] and IADS sound[2] [*disgust*: valence mean ± SD = 4.00 ± 1.72, arousal mean ± SD = 5.82 ± 1.93; *fear*: valence mean ± SD = 4.00 ± 1.72, arousal mean ± SD = 5.82 ± 1.93; *sadness*: valence mean ± SD = 3.28 ± 1.65, arousal mean ± SD = 6.61 ± 1.89] were selected and combined together according to their arousal and valence values provided in the databases. For example, a negative/high aroused sound was matched with a negative/high aroused image. On the other hand, the emotions happiness, surprise, and anger were elicited using video clips. A pilot study was conducted to identify the video clip that was better able to elicit the target emotion in the participants. 90 video clips corresponding to happiness, surprise and anger were displayed to 30 volunteers with a mean age of 26.4 years (ranging from 24 to 45 years). All of them were psychology teachers or students of the UKM medical center, Kuala Lumpur. Of these, 30 clips with the highest ratings were chosen for data collection.

3.5 . Emotion elicitation protocol

An illustrated representation of the emotion elicitation protocol is shown in Fig. 1(a). As shown in the figure, the protocol had two sessions of three trials each. There was a break of 10–15 min between the sessions. The participants were allowed to relax during the break since the continuous assessment would have been too exhausting. The multimodal stimuli relating to all the six emotional states (happiness, sadness, fear, anger, surprise and disgust) were displayed in each trial in a random order. Each combination of picture and sound was presented for 6 s (Yuvaraj et al., 2014). To maximize the participants' emotional

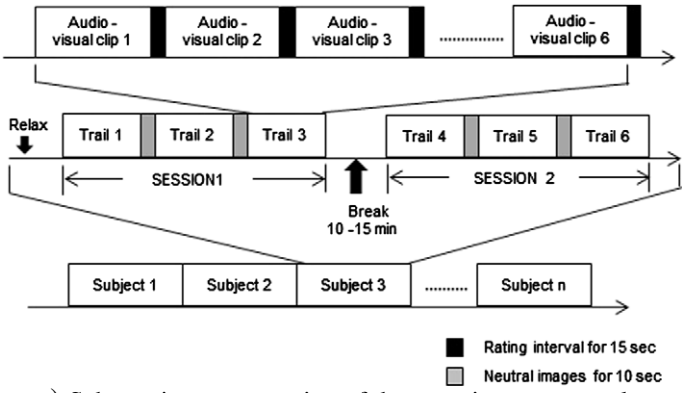

a) Schematic representation of the experiment protocol

b) Experimental setupfor emotion assessment using multimodal stimuli

S. NO	Audio-visual clip No.	Primary emotion experienced (✓)						Intensity of primary emotion (✓)					Any other emotion ? (✓)					
		HAPPY	SAD	FEAR	ANGER	SURPRISE	DISGUST	VERY LOW	LOW	MEDIUM	HIGH	VERY HIGH	HAPPY	SAD	FEAR	ANGER	SURPRISE	DISGUST
1	Clip 1																	
2	Clip 2																	
3	Clip 3																	
4	Clip 4																	
5	Clip 5																	
6	Clip 6																	
7	Clip 7																	
8	Clip 8																	
9	Clip 9																	
10	Clip 10																	
11	Clip 11																	

c) Self-assessment questionnaire

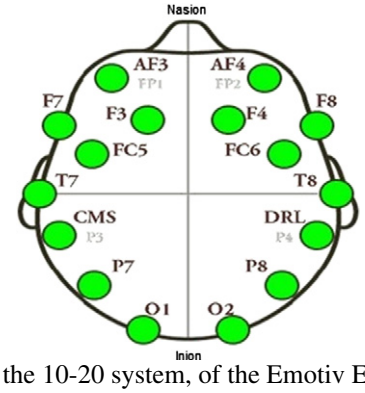

d) Electrode positions, according to the 10-20 system, of the Emotiv EPOC device used for EEG acquisition.

Fig. 1. (a) Schematic representation of the experiment protocol. (b) Experimental setup for emotion assessment using multimodal stimuli. (c) Self-assessment questionnaire. (d) Electrode positions, according to the 10–20 system, of the Emotiv EPOC device used for EEG acquisition.

response, each clip block consisted of six combinations of the same emotional category and lasted for 36 s. In addition, each of the video clips varied from 36 and 45 s in duration, depending on the length of the clip. Neutral images, which can calm down the participants, were displayed for 10 s at the start of each trial. This would help the participants return to the normal or neutral state away from emotional excitation. Besides, a 15 second rating interval (Hamdi et al., 2012) was provided between the clips in which participants answered a five-point self-assessment questionnaire. Each session took approximately 30 min.

3.6 . Procedure

The purpose of the study was clearly explained to the participants before initiating the experiment. The participants were further requested to relax, minimize their bodily movements (as much as possible, to reduce the appearance of undesired artifacts in the EEG recordings), and concentrate on the emotional stimuli. The self-guided emotion elicitation protocol was then displayed on the screen. The complete experimental setup is shown in Fig. 1(b). At the end of each clip, participants filled a self-assessment questionnaire to state the status of the emotions they felt during the experiment; they were also asked to report the strength of the emotions using a five-point scale according to the degree (1 = very low, 2 = low, 3 = medium, 4 = high, and 5 = very high). These ratings were then used to understand the intensity of the emotional state they experienced. However, despite the intensity levels, all emotional data were taken into considerations. The participants were also allowed to indicate multiple emotions during the experiment. An example of the self-assessment questionnaire is shown in Fig. 1(c).

3.7 . EEG recordings

EEG recordings were conducted using the Emotive EPOC 14 channel EEG wireless recording headset (Emotive Systems, Inc., San Francisco, CA) (Hadjidimitriou and Hadjileontiadis, 2012). The electrode scheme was arranged according to the international 10–20 system and included active electrodes at AF3, F7, F3, FC5, T7, P7, O1, O2, P8, T8, FC6, F4, F8, and AF4 positions, referenced to the common mode sense (CMS-left mastoid)/driven right leg (DRL-right mastoid) ground as shown in Fig. 1(d). The acquired data were digitized using the embedded 16-bit ADC with 128 Hz sampling frequency per channel and sent to the computer via wireless communication, which utilizes a proprietary USB dongle to communicate using the 2.4 GHz band.

4 . Methods

4.1 . Signal preprocessing

First, the time waves of EEG data were pre-processed using thresholding method to remove movement artifacts (such as eye movement/blinking), in which data that are found to have amplitudes of more than 80 μV are discarded from the study (Gotlib et al., 1998). Second, a 6th order bandpass Butterworth filter (with forward reverse filtering algorithm) was used to extract the frequency range of 1–49 Hz. Third, each channel of the artifact-free emotional EEG data was divided into same-length of epochs without overlapping using time windows. Finally, all features discussed below were computed on each epoch of the emotional EEG data of PD patients and HC.

4.2 . Feature extraction

The main task of feature extraction is to derive the significant features which can map the EEG data into consequent emotional states. For a comparative study, we investigated four kinds of features, namely bispectrum, power spectrum, wavelet packet and nonlinear dynamical analysis.

4.2.1 . Bispectrum feature

Higher order spectra are the spectral representations of higher order moments or cumulants of a signal (Nikias and Petropulu, 1993). The third order statistics is called bispectrum which is used in this study. The bispectrum $B(f_1, f_2)$ is the Fourier transform of the third order correlation of the signal and is given by

$$B(f_1, f_2) = E\left[X(f_1)X(f_2)X^*(f_1 + f_2)\right] \quad (1)$$

where $X(f)$ represents the Fourier transform of the signal $x(nT)$, n is an integer index, * denotes complex conjugate and $E[\,]$ denotes the statistical expectation operation over an ensemble of possible realizations of the signal. For deterministic sampled signals, $X(f)$ is the discrete-time Fourier transform and is computed using Fast Fourier Transform (FFT) algorithm. The frequency f may be normalized by the Nyquist frequency (half of the sampling frequency) that lies between 0 and 1. The bispectrum, given by Eq. (1), is a complex valued function of two frequencies. The bispectrum exhibits symmetry, and needs to be computed in non-redundant regions or in its principal domain. Assuming there is no bispectral aliasing, the bispectrum of a real valued signal is uniquely defined with the triangle $0 \le f_2 \le f_1 \le f_1 + f_2 \le 1$. This non-redundant region is denoted by Ω, which is also termed as principal domain and is shown in Fig. 2 (Nikias and Petropulu, 1993).

In order to calculate bispectrum feature, we used epochs of 768 samples with Hanning window of 50% overlap corresponding to 6 s at the used sampling rate of 128 Hz. These epochs were taken from each record of 1024 NFFT points. The mean magnitude of the bispectrum were log transformed after being extracted in standard EEG frequency bands such as *delta* (1–4 Hz), *theta* (4–8 Hz), *alpha* (8–13 Hz), *beta* (13–30 Hz) and *gamma* (30–49 Hz). Besides the bispectrum feature of all electrodes (BNoAs), the bispectrum of the hemispheric asymmetry index was also chosen as features. Throughout the whole brain, there were seven asymmetry indices derived from seven symmetric electrode pair combinations, namely AF3–AF4, F7–F8, F3–F4, FC5–FC6, T7–T8, P7–P8, and O1–O2. The asymmetry indices were calculated either by bispectrum subtraction (e.g. bispectrum of F3 minus bispectrum of F4) or division (bispectrum of F3 divided by bispectrum of F4) (Lin et al., 2010; Wang et al., 2013) and named as bispectrum differential asymmetry of seven electrode pairs (BDAs) and rational asymmetry of seven electrode pairs (BRAs), respectively.

4.2.2 . Power spectrum feature

Power spectrum (second order measures of HOS) can be analyzed to characterize the perturbations in the oscillatory dynamics of ongoing EEG (Lin et al., 2010). First, each of the EEG data was processed with the Hanning window in order to reduce 'spectral leakage effects'. Second, the windowed epochs were subjected to Fast Fourier Transform (FFT) with length of 1024 points (spectral resolution of 0.125 Hz). Finally, EEG power spectra were log transformed after being extracted in *delta*, *theta*, *alpha*, *beta*, and *gamma* bands with ranges as mentioned previously. Similar to the bispectrum asymmetry, we also adopted the

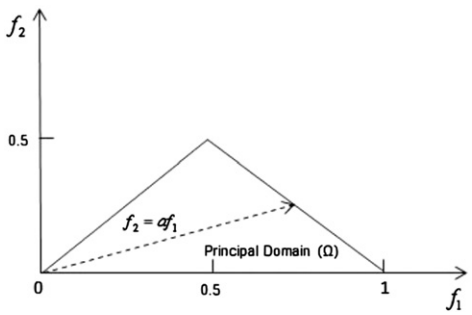

Fig. 2. Non-redundant region (Ω) of computation of the bispectrum for real signals.

spectral power of the hemispheric asymmetry and labeled as power spectrum differential asymmetry (PDAs) and rational asymmetry (PRAs) of seven electrode pairs (Lin et al., 2010; Wang et al., 2013).

4.2.3 . Wavelet packet (WP) feature

Wavelet packet feature is the time–frequency domain feature that has been used for EEG signal analysis (Murugappan et al., 2010). Usually, tests are performed with different types of wavelets and the one which gives maximum efficiency is selected for the particular application. In this study, Daubechies wavelet of order four (db4) was used to analyze the emotional EEG data. In order to investigate the effect of other wavelets on classification accuracy, tests were carried out using other wavelets. Apart from db4, Symmlet of order 10 (sym10), Coiflet of order 4 (coif4), and Daubechies of order 2 (db2) were also tested. It was noticed that the daubechies wavelet gives best accuracy (due to its near optimal time–frequency location properties) than the others, and db4 is slightly better than db2.

Furthermore, the choice of number of decomposition level is very important in the analysis of signals using WP transform (WPT). The decomposition level is chosen based on the dominant frequency components of the signal. The level(s) are chosen such that those parts of the signal that correlate well with the frequency necessary for classification of the signal are retained in the wavelet packet coefficients. In the present study, EEG signals were decomposed into four levels. The lowest frequency resolution can be estimated as

$$\Delta f = \frac{1}{2^4}\frac{f_s}{2} = 4\text{Hz} \tag{2}$$

where f_s is the sampling rate of 128 Hz. There are $2^4 = 16$ sub-bands of wavelet packets at the fourth level whose corresponding frequency ranges are $f_1 : [0, 4], f_2 : [4, 8], f_3 : [8, 12], f_4 : [12, 16],\ldots, f_{16} : [60, 64]$. These frequency bands have similar range with the traditional frequency bands derived from clinical EEG signal analysis. Specifically, the *delta* band is f_1: 1–4 Hz, the *theta* band is f_2: 4–8 Hz, the *alpha* band is f_3: 8–12 Hz, the *beta* band is $f_4 - f_8$: 12–32 Hz and the *gamma* band is $f_9 - f_{16}$: > 32 Hz. Thus specific bands of emotional EEG signals can be extracted by WPT from PD patients and HC.

Since the coefficients from each resolution level j correspond to different frequency bands, the energy E_j for each frequency range in each time window can be computed as the corresponding squared coefficients. Total energy E_{total} of the signal in each time window was calculated as the sum of energies of all resolution levels. Thereafter, the relative wavelet energy (RWE) (Eq. (3)) was computed as the ratio between the energy of each band.

$$P_j = E_j / E_{total} \tag{3}$$

Then, the wavelet packet entropy (WPE) can be defined as

$$\text{WPE}_j = -\sum_j P_j \log_2 P_j \tag{4}$$

The relative wavelet coefficient energy P_j, and wavelet packet entropy WPE_j were chosen as the time–frequency domain features in this study.

4.2.4 . Nonlinear feature

Nonlinear analysis is useful for biological time series (such as EEG) analysis as such signals typically exhibit complex dynamics (Aftanasa et al., 1997). Several nonlinear features approaches have been proposed to detect the underlying important dynamical properties of the physiological phenomenon. In this paper, we studied the emotional EEG signals using three different types of nonlinear dynamical features, namely approximate entropy, Hurst exponent, and detrended fluctuation analysis.

Approximate entropy (A_e) is part of a family of statistics that can be seen as nonlinear quantification of the regularity of a signal (Pincus, 1995). Approximate entropy takes into account the temporal order of points in a time sequence and is therefore appropriate measure of randomness or regularity. The first step in computing approximate entropy of a time series x_i, $i = 1, 2,\ldots..., n$, is to construct the state vectors in the embedding space:

$$y_i = \left\{x_i, x_{i+1}, x_{i+2}, \ldots..., x_{(i+m-1)}\right\}, 1 \le i \le n-m+1 \tag{5}$$

where m is the embedding dimension. Second, we compute

$$C_i^m(r) = \frac{1}{n-m+1}\sum_{j=1}^{n-m+1}\theta\left(r - d\left(y_i, y_j\right)\right) \tag{6}$$

where $\theta(y)(\theta(y) = 1)$ for $y > 0$, $\theta(y) = 0$, otherwise) is the standard Heavyside function, r is the vector comparison distance, and $d(y_i, y_j)$ is a distance measure defined by

$$d\left(y_i, y_j\right) = \max_{k=1,2,\ldots,m}\left(\left|y_{i+k-1)} - y_{j+k-1)}\right|\right) \tag{7}$$

$$\text{Third, we compute } \phi^m(r) \text{ as}, \phi^m(r) = \frac{1}{n-m+1}\sum_{i=1}^{n-m+1}\ln C_i^m(r) \tag{8}$$

Finally, for fixed m, r, and n, approximate entropy A_e can be expressed as

$$A_e(m, r, n) = \phi^m(r) - \phi^{m+1}(r) \tag{9}$$

For this study, m is set to 2 and r is set to 0.2 times of the standard deviation of the data. These values are selected on the basis of previous studies indicating good statistical validity for A_e using these values (Pincus and Goldberger, 1994).

Hurst exponent (H) is the measure of the smoothness of a fractal time series based on the asymptotic behavior of the rescaled range of the process. In time series analysis, the Hurst exponent is used by many researchers for characterizing the non-stationary behavior of the EEG episodes (Wang et al., 2013). First, the accumulated deviation of mean of the time series over time is computed. The rescaled range R/S follows a power law relationship with time T as,

$$R/S \sim T^H \tag{10}$$

where R is the difference between the maximum and minimum deviation from the mean and S represents the standard deviation. The Hurst exponent, H can be derived as,

$$H = \log(R/S)/\log(T) \tag{11}$$

where T is the length of sample data and R/S represents the corresponding value of rescaled range.

In addition, in this work we also used detrended fluctuation analysis (DFA), which is a method for determining the statistical self-affinity of a signal. It is related to measures based upon spectral techniques such as autocorrelation and Fourier transform. Briefly, the time series to be analyzed (with N samples) is first integrated. Next, the integrated time series is divided into boxes of equal length, n. In each box of length n, a least square line is fit to the data (representing the trend in that box). The y coordinate of the straight line segments is denoted by $y_n(k)$. Next, we detrended the integrated time series, $y(k)$, by subtracting the local trend, $y_n(k)$, in each box. The root mean-square

fluctuation of this integrated and detrended time series was calculated by

$$F(n) = \sqrt{\frac{1}{N}\sum_{k=1}^{N}[y(k) - y_n(k)]^2} \quad (12)$$

4.3 . Feature dimensionality reduction

Feature dimensionality reduction cannot only improve learning efficiency, but also improve prediction performance. In this study, feature dimensionality reduction was carried out with three well known dimension reduction methods, namely principal component analysis (PCA), independent component analysis (ICA), and correlation-based feature selector (CFS).

The principal component analysis is a useful statistical technique that represents the raw data in a lower dimensional feature space to convey maximum useful information, by seeking to find the highest variability in the original feature space. It uses eigenvalues to determine the significance of principal components so that dimensionality reduction is accomplished by selecting principal components in accordance with magnitude of their associated eigenvalues. Independent component analysis is a nonlinear dimensionality reduction method (Hyvarinen and Oja, 2000). It assumes that the observed signal is a result of mixing of several sources or independent signals. The ICA method involves computation of a mixing matrix. The weights in this mixing matrix are used as features for subsequent emotion pattern classification.

Correlation-based feature selector is a kind of supervised dimensionality reduction method. Each feature gets a score presenting its correlation with emotion by this method. The most emotion-relevant features can be found by ranking these scores. Let EEG feature set be denoted by $m \times n$ matrix X, where m is the dimension of features and n is the number of samples, then $X = \{X_1, X_2, \ldots\ldots X_n\}$. Let r_i^T denote the random variable corresponding to the *ith* component of X, $i = 1, 2, 3, \ldots. m$ and y denote the label set of samples. The emotion-relevant score of each feature can be computed as follows:

$$R_{r_i y} = \frac{C_{r_i y}}{\sqrt{C_{r_i} C_y}} \quad (13)$$

where C represents covariance and R denotes the correlation coefficient. The absolute value of correlation can be regarded as the emotion-relevant score. Ranking these scores in a descending order, the top-ranked features are considered as the most emotion-relevant features.

4.4 . Emotional state classification

To assess the association between EEG and emotional states of PD patients in comparison with HC, the classification into the predefined emotional classes was achieved by using support vector machine (SVM) classifiers and Fuzzy K-Nearest Neighbor (FKNN).

In SVM, a separating hyperplane that maximizes the margin between the input data classes which are viewed in an n-dimensional space (n is the number of features used as inputs) is determined. SVM can be easily adapted to nonlinearly separable data by the use of kernel functions to map the data to a much higher dimensional space where the data becomes more separable. FKNN assigns a class based on the predominant class among the k nearest neighbors. Euclidean distance was used as the metric in FKNN allocating fuzzy class memberships before making decisions. The fuzzy strength parameter m is used to determine how heavily the distance is weighted when calculating each neighbor's contribution to the membership value. Here, the m value is varied between 1 and 2 with steps of 0.01, and the classification performance is obtained using k-values between 1 and 10.

In order to use entire dataset for training and testing the classifiers, a ten-fold cross-validation method was adopted, where the feature vectors were divided randomly into ten sets and training is repeated for ten times. Classification performance was evaluated through the classification accuracy (CA) and is computed between six emotional states of PD patients and HC as,

$$\%\text{Accuarcy}_{Emotion} = \frac{\text{Number of correctly classified feature vectors}_{Emotion}}{\text{Total number of tested feature vectors}_{Emotion}} \times 100\% \quad (14)$$

where *Emotion* refers to the six emotional states namely happiness, sadness, fear, anger, surprise and disgust of PD patients and HC (i.e., PD patients$_{(happiness\ vs\ sadness\ vs\ fear\ vs\ anger\ vs\ surprise\ vs\ disgust)}$, and HC$_{(happiness\ vs\ sadness\ vs\ fear\ vs\ anger\ vs\ surprise\ vs\ disgust)}$), across delta, theta, alpha, beta, gamma EEG frequency bands and ALL (combination of five frequency bands). The overall performance of the classifier is evaluated by taking the average and standard deviation (SD) of the accuracies of the ten-fold classification. Here, the SD of the classification clearly reveals the consistency of the classifier results and the number of classes used for classification here is six for each group.

4.5 . Trajectory of emotion changes

In the analysis, we focused on the emotion classification, but then emotion usually changes. Thus we also used manifold learning to find the trajectory of emotion changes in PD patients and HC.

In this work, the Isometric feature mapping method (hereafter referred as Isomap) is chosen for its global characteristics (Tenenbaum et al., 2000). Isomap has been successfully applied to the analysis of high-dimensional biomedical data (Park, 2012). Isomap seeks to preserve the intrinsic geometry of the nonlinear data by utilizing the geodesic manifold distances (i.e. shortest path along the manifold connecting two points) between all pairs of data points (Balasubramanian and Schwartz, 2002). The algorithm can be summarized in three steps: Step 1: Construction of global neighborhood graph. For each point, find its k nearest neighbors using the predefined conditions. Construct a neighborhood graph by connecting each point to its k neighbors, with the distance of the points in the original spaces as the edge weights. Step 2: Computation of shortest paths. Estimate the shortest paths $d_{i,j}$ between each pair of points i, j as geodesic distance. The shortest paths were computed by Dijkstra method with the global neighborhood graph. Step 3: Construction of embedding. After calculation of the shortest paths, the data can be represented with the matrix $D = \{d_{i,j}^2\}$, expressing the geodesic distance of each pair of points on the manifold. Applying classical multidimensional scaling (MDS) to this matrix constructs an embedding of the data that best preserves the manifolds estimated intrinsic geometry.

$$\text{Assume that } K = -\frac{1}{2}\left(I - zz^T\right)D\left(I - zz^T\right), \quad (15)$$

with $z = 1/n(1, 1, \ldots.1)^T$. The largest k eigenvalues of K are $\lambda_1, \lambda_2, .., \lambda_k$ and the respective eigenvectors are $u_1, u_2, \ldots. u_k$. Assume $U = (u_1, u_2, \ldots., u_k)$, then the embedding result is

$$Y = diag\left(\sqrt{\lambda_1}, \sqrt{\lambda_2}, \ldots., \sqrt{\lambda_k}\right)U^T \quad (16)$$

The selected features we obtained from dimensionality reduction were input to the Isomap model and the one dimension output curve is the trajectory of the emotional changes.

Table 2
Average classification accuracies (±standard deviation) of bispectrum feature (BNoAs) across different EEG frequency bands with different length time windows using SVMRBF.

Time windows length	Group	Emotional EEG frequency band					
		Delta (%)	Theta (%)	Alpha (%)	Beta (%)	Gamma (%)	ALL (%)
2 s	PD	49.89 ± 2.27	46.53 ± 2.49	56.02 ± 3.54	74.86 ± 1.10	72.12 ± 1.78	77.20 ± 2.81
	HC	51.93 ± 2.16	52.78 ± 2.54	61.34 ± 2.30	78.24 ± 2.17	74.50 ± 2.67	80.39 ± 2.13
3 s	PD	47.36 ± 2.05	44.91 ± 2.01	51.32 ± 1.84	75.30 ± 2.67	74.00 ± 1.78	74.93 ± 1.55
	HC	50.76 ± 2.58	51.62 ± 2.27	60.42 ± 2.23	78.52 ± 1.83	76.55 ± 2.16	78.37 ± 1.34
5 s	PD	52.66 ± 2.53	48.96 ± 1.80	59.47 ± 1.99	75.42 ± 1.91	74.09 ± 2.64	76.58 ± 2.21
	HC	54.24 ± 2.01	56.17 ± 2.19	67.45 ± 2.21	79.07 ± 1.79	78.31 ± 1.82	81.48 ± 1.84
6 s	PD	53.29 ± 2.23	50.76 ± 2.50	64.88 ± 2.37	76.97 ± 1.91	74.72 ± 2.24	77.43 ± 1.59
	HC	55.05 ± 2.45	57.25 ± 3.11	72.50 ± 1.85	80.30 ± 1.95	78.84 ± 2.05	83.04 ± 1.87
8 s	PD	51.60 ± 2.10	47.45 ± 3.10	54.49 ± 2.42	74.88 ± 1.01	73.45 ± 3.02	74.01 ± 1.82
	HC	52.70 ± 1.63	57.01 ± 1.69	57.92 ± 2.04	75.57 ± 1.76	75.00 ± 2.01	80.76 ± 2.12

Note: Here, 'ALL' means the combination of five EEG frequency band bispectrum features. Due to space reasons we have reported only the top five classification accuracies of different length time windows.

5 . Experimental results and discussions

5.1 . Statistical analysis

The statistical significance of all the computed emotion-specific features (namely bispectrum [BNoAs, BDAs, and BRAs], power spectrum [PNoAs, PDAs, and PRAs], wavelet packet [WPE, and RWE] and nonlinear dynamical analysis [A_e, H, and DFA]) was studied using analysis of variance (ANOVA) test. The significant threshold was set to ($p < 0.05$). The ANOVA results indicated that all the emotion features showed statistically significant ($p < 0.05$) changes among the six emotional states of PD patients and HC across delta, theta, alpha beta, gamma and ALL frequency bands. This also ensures the probability of achieving better classification accuracy. In particular, emotional features of HC show very low p-value ($p < 0.0001$) compared to PD ($p < 0.05$) among the six emotional states. This may ensure that the EEG is not reflecting the emotion accurately in PD, which could be interpreted as impairment in the brain's processing ability of emotions.

5.2 . Time windows

To find the most suitable time window length, we compared the classification performance using bispectrum feature (BNoAs) obtained from PD patients and HC across different EEG frequency bands with ten different length time windows between 1 s and 10 s in step of 1 s. The radial basis function (RBF) kernel SVM classifier was applied to these ten different lengths. The average classification results are presented in Table 2. It can be seen that the average classification of accuracy of 6 s EEG epochs is better than those of the others. Hence 6 s was chosen as the time window length in the remaining analysis. Fig. 3 shows the average classification accuracies of bispectrum across the delta, theta, alpha, beta, gamma and ALL frequency bands with different length time windows for PD patients and HC. In this case, twenty participants from each group with six emotions, six trials per emotion, and six epochs per channel for each band resulted in a total of 4320 × 70 (14 channels × 5 bands) feature vectors, which were processed.

5.3 . Choosing of SVM kernels

One of our motivations is to obtain the best classification performance of emotional states of PD patients and HC. For the SVM classifier, to find the best kernel, the performance of three different types of kernels, namely linear kernel (hereafter denoted SVMlinear), polynomial kernel (SVMpoly), and RBF kernel (SVMRBF), was compared in our experiments. The parameters of SVM were determined by ten-fold cross-validation technique. For SVMlinear, we estimated the classification accuracy using different cost parameters C: $C \in \{2^{-5}, 2^{-4}, \ldots, 2^{14}, 2^{15}\}$. For SVMpoly, we studied the validation accuracy using different combinations of the cost parameter C and polynomial degree of d: $C \in \{2^{-5}, 2^{-4}, \ldots, 2^{14}, 2^{15}\}$ and $d \in \{1, 2, 3, \ldots, 14, 15\}$. For SVMRBF, we used the different combinations of the cost parameter C and kernel parameter γ: $\gamma \in \{2^{-15}, 2^{-14}, \ldots, 2^{3}, 2^{4}\}$. The code to implement SVMs was obtained from LibSVM (Chang and Lin, 2001).

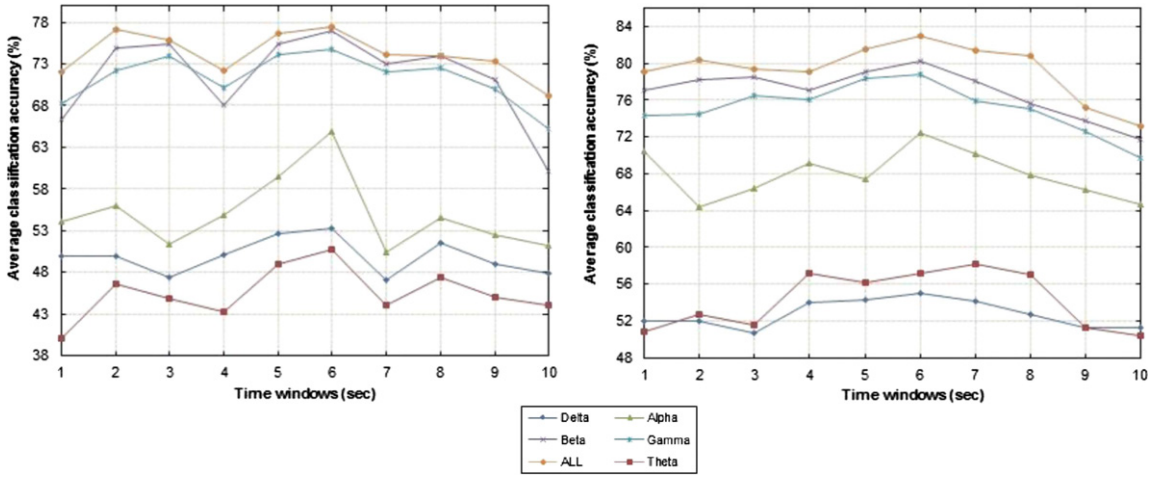

Fig. 3. Average classification accuracies of bispectrum feature across EEG bands with different length time windows. (a) PD patients (b) healthy controls.

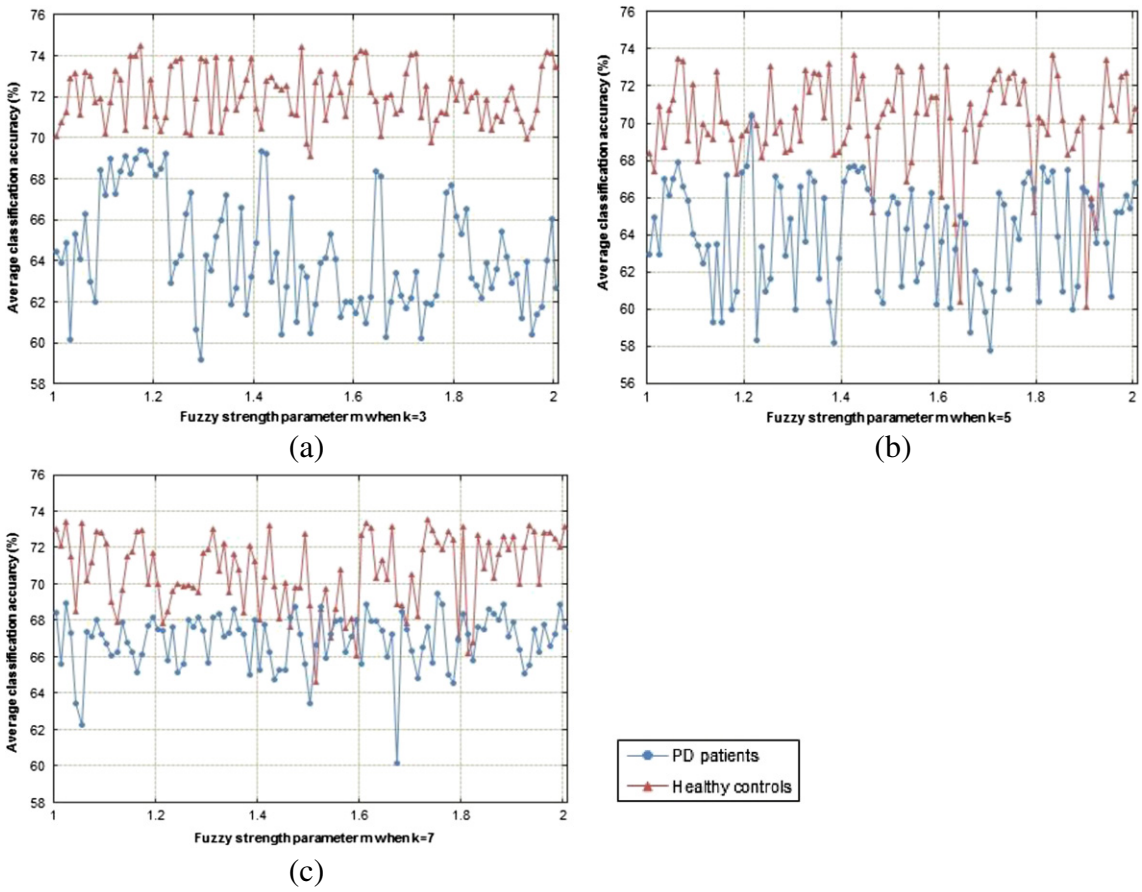

Fig. 4. The relationship between average classification accuracy of bispectrum feature across ALL EEG frequency bands and fuzzy strength m with different numbers of *k*.

Fig. 4 shows the relationship between the FKNN classification accuracy of bispectrum across ALL frequency bands and fuzzy strength parameter *m* which varies in the range of 1 and 2 in the steps of 0.01 using different values of *k*. It can be observed that the classification accuracy fluctuates between 60% and 75% with different values of *m*. It reveals that the fuzzy strength parameter has a big impact to the performance of FKNN classifier. The better classification accuracy was achieved with the parameter pair of (3, 1.17), (5, 1.06), and (7, 1.02) as shown in Fig. 4(a)–(c) when *k* is equal to 3, 5, and 7 respectively. These optimal different parameter pairs, namely (3, 1.17), (5, 1.06), and (7, 1.02) are used in the subsequent experiments, and for convenience they are named FKNN1, FKNN2, and FKNN3 respectively.

Tables 3 and 4 show the average classification performance of bispectrum feature extracted from PD patients and healthy controls' emotional states across the delta, theta, alpha, beta, gamma, and ALL frequency bands using SVM (linear, poly, and RBF kernels) and FKNN classifier (FKNN1, FKNN2, and FKNN3). From the tables, several important observations can be drawn. *First*, it can be observed that the classification performance of bispectrum across ALL frequency bands is better than those based on individual frequency bands under the same conditions. *Second*, it is found that the classification performance of the alpha, beta, and gamma bands is better than those of delta and theta bands in both groups. This partly reflects that higher frequency bands play a more important role in emotion activities than lower frequency bands (Oathes and Ray, 2008; Wang et al., 2013) in PD patients and HC respectively. On the contrary, previous findings of EEG–emotion correlation in theta band has been reported (Aftanas and Golocheikine, 2001; Sammler et al., 2007). This may be influenced by the contribution of different approaches to data analysis. *Third*, PD patients achieved less averaged classification performance compared with HC among the six emotional states. This suggests that the PD patients give lower accuracy as the EEG is not representing the emotion accurately, which could be interpreted as impairment in the brain's processing ability of emotions. This is an agreement with other studies that there is decrease in brain's complexity during emotion processing due to the dysfunction in the neural circuits (Adolphs et al., 1996; Lawrence et al., 2007). Recent evidence points to neuropathological changes in PD in many brain areas which are assumed to play key roles in emotion processing (Kober

Table 3
Average classification accuracies (±standard deviation) of bispectrum feature (BNoAs) across different frequency bands using SVM with different kernels.

Kernel function	Group	Emotional EEG frequency band					
		Delta (%)	Theta (%)	Alpha (%)	Beta (%)	Gamma (%)	ALL (%)
Linear	PD	46.50 ± 1.91	38.75 ± 1.48	43.68 ± 2.19	48.13 ± 1.21	50.16 ± 2.35	56.76 ± 1.25
	HC	50.51 ± 1.92	46.55 ± 1.89	53.75 ± 2.06	56.18 ± 2.27	59.38 ± 1.93	61.30 ± 2.16
Poly	PD	48.66 ± 2.46	39.03 ± 1.12	55.12 ± 2.18	60.53 ± 1.83	61.83 ± 3.00	68.13 ± 2.08
	HC	52.89 ± 1.63	47.66 ± 2.28	59.12 ± 1.62	67.92 ± 2.28	71.62 ± 1.26	72.52 ± 1.55
RBF	PD	53.29 ± 2.23	50.76 ± 2.50	64.88 ± 72.50	76.97 ± 1.91	74.72 ± 2.24	77.43 ± 1.59
	HC	55.05 ± 2.45	57.25 ± 3.11	64.88 ± 2.37	80.30 ± 1.95	78.84 ± 2.05	83.04 ± 1.87

Note: Here, 'ALL' means the combination of five EEG frequency band bispectrum features.

Table 4
Average classification accuracies (±standard deviation) of bispectrum feature (BNoAs) across different frequency bands using FKNN with different optimal parameters.

FKNN	Group	Emotional EEG frequency band					
		Delta (%)	Theta (%)	Alpha (%)	Beta (%)	Gamma (%)	ALL (%)
FKNN1	PD	49.17 ± 2.59	41.00 ± 2.37	47.55 ± 2.77	62.59 ± 1.79	62.66 ± 1.94	69.42 ± 1.56
k = 3	HC	54.56 ± 1.99	51.06 ± 2.71	57.20 ± 1.86	70.79 ± 1.41	72.22 ± 2.86	74.46 ± 1.75
m = 1.17							
FKNN2	PD	46.94 ± 2.09	38.89 ± 1.57	46.18 ± 2.52	58.36 ± 1.49	60.37 ± 2.74	67.69 ± 2.62
k = 5	HC	51.76 ± 2.01	49.38 ± 1.70	53.75 ± 2.06	69.63 ± 1.92	71.88 ± 2.01	73.50 ± 1.27
m = 1.06							
FKNN3	PD	47.45 ± 1.50	40.81 ± 2.35	36.44 ± 1.89	60.83 ± 2.00	60.56 ± 1.45	68.98 ± 2.24
k = 7	HC	53.96 ± 2.33	49.49 ± 3.39	45.00 ± 0.87	69.55 ± 1.68	72.06 ± 2.12	73.38 ± 1.59
m = 1.02							

Note: Here, 'ALL' means the combination of five EEG frequency band bispectrum features.

Table 5
Average classification accuracies (±standard deviation) of bispectrum asymmetry feature across different frequency bands using SVM with RBF kernel.

Feature type	Group	Emotional EEG frequency band					
		Delta (%)	Theta (%)	Alpha (%)	Beta (%)	Gamma (%)	ALL (%)
BDAs	PD	46.85 ± 2.02	48.24 ± 1.82	52.15 ± 1.31	68.63 ± 1.99	65.00 ± 1.49	72.96 ± 1.56
	HC	50.97 ± 2.46	52.50 ± 2.33	52.87 ± 2.63	67.62 ± 1.74	67.20 ± 3.02	74.31 ± 2.19
BRAs	PD	47.11 ± 1.83	49.21 ± 2.86	52.38 ± 2.26	68.50 ± 1.89	64.95 ± 1.53	73.82 ± 1.70
	HC	50.32 ± 2.32	53.15 ± 2.71	53.15 ± 2.28	67.94 ± 1.40	66.27 ± 2.02	73.84 ± 1.70

Note: Here, 'ALL' means the combination of five EEG frequency band bispectrum features.

et al., 2008). These include limbic structures such as the amygdala, and the ventral striatum, which is centrally located within the basal ganglia's limbic loop. Furthermore, our results are compatible with the more general hypothesis that a loss of complexity appears when the biological systems become functionality impaired (Jeong et al., 1998). *Finally*, the average classification performance of SVM with RBF kernel outperforms SVMlinear, SVMpoly and FKNN classifier. The best average classification accuracy of bispectrum across ALL frequency bands using SVMRBF is 77.43% ± 1.59% and 83.04% ± 1.87% for PD patients and HC, respectively. This definitely proves the robustness of the SVMRBF over the SVMlinear, SVMpoly and FKNN for these data sets. Therefore SVM with RBF kernel was chosen as the classifier for the following stages.

5.4 . Comparison of bispectrum with other features

To find the best emotion-specific features of PD patients and HC, the other types of features were also analyzed in this study. Table 5 shows the average classification performance of the bispectrum differential and rational asymmetry features. It can be seen that the classification performance of the combination of ALL bispectrum of differential asymmetry is better than BRAs features. The average accuracy with the combination of ALL BDAs features is 72.96% ± 1.56% and 74.31% ± 2.19% for PD patients and HC, respectively using SVMRBF kernel function. Table 6 shows the average classification performance of power spectrum feature types PNoAs, PDAs, and PRAs across different EEG frequency bands. The classification performance of using PNoAs is evidently better than those based on other types under the same conditions. A maximum average classification accuracy of 65.62% ± 2.56% and 68.19% ± 2.34% is obtained using ALL frequency bands for PD patients and HC, respectively.

Table 7 shows the classification performance of the WP features. The average classification performance of wavelet packet entropy across ALL frequency bands is better than other wavelet packet feature. A maximum classification accuracy of 55.97% ± 1.77% and 63.96% ± 2.61% for PD patients and HC respectively is obtained using the WP entropy across ALL frequency bands. Table 8 shows the classification performance using nonlinear dynamical features. From Table 8, it can be seen that the approximate entropy feature gives a maximum average classification accuracy of 67.61% ± 1.36% and 73.17% ± 1.57% for PD patients and HC, respectively over other nonlinear dynamical features.

From the above analysis, the average classification performance confirms that bispectrum across ALL frequency bands is the most robust feature among all of the four types of features studied.

5.5 . Comparison of feature dimensionality reduction methods

Our goal here was to find the relationship between EEG data and emotional states of PD patients in comparison with HC. Moreover, we wished to obtain the general subject-independent features related to emotion. Thus, feature dimensionality reduction was implemented in our study. Since the best performance was obtained using the bispectrum across ALL frequencies, three kinds of dimensionality reduction methods, namely PCA, ICA and CFS were applied for further data analysis.

Table 6
Average classification accuracies (±standard deviation) of power spectrum feature across different frequency bands using SVM with RBF kernel.

Feature type	Group	Emotional EEG frequency band					
		Delta (%)	Theta (%)	Alpha (%)	Beta (%)	Gamma (%)	ALL (%)
PNoAs	PD	47.08 ± 1.36	40.44 ± 2.47	46.76 ± 2.57	61.81 ± 2.30	58.86 ± 1.81	65.62 ± 2.56
	HC	53.36 ± 1.82	50.37 ± 2.83	55.00 ± 1.57	69.86 ± 1.78	66.83 ± 1.40	68.19 ± 2.34
PDAs	PD	41.83 ± 1.96	34.84 ± 1.53	43.73 ± 2.02	48.89 ± 1.65	42.36 ± 1.80	52.82 ± 2.55
	HC	47.27 ± 2.13	43.87 ± 1.59	48.73 ± 1.98	53.08 ± 2.78	47.85 ± 1.68	56.83 ± 2.05
PRAs	PD	38.13 ± 2.62	33.52 ± 1.48	36.37 ± 2.21	48.19 ± 2.19	40.12 ± 2.95	49.56 ± 2.67
	HC	42.96 ± 3.14	37.20 ± 1.54	40.65 ± 2.40	49.95 ± 2.46	42.34 ± 1.54	54.93 ± 3.32

Note: Here, 'ALL' means the combination of five EEG frequency band power spectrum features.

Table 7
Average classification accuracies (±standard deviation) of wavelet packet feature across different frequency bands using SVM with RBF kernel.

Wavelet feature	Group	Emotional EEG frequency band					
		Delta (%)	Theta (%)	Alpha (%)	Beta (%)	Gamma (%)	ALL (%)
RWE	PD	19.44 ± 1.56	18.87 ± 1.06	39.81 ± 2.27	40.76 ± 2.44	42.48 ± 1.98	49.47 ± 1.67
	HC	28.06 ± 2.24	27.85 ± 2.02	47.87 ± 0.97	50.12 ± 1.72	49.10 ± 1.66	59.07 ± 2.18
WPE	PD	41.50 ± 2.68	30.67 ± 1.34	41.97 ± 2.59	46.30 ± 2.91	45.93 ± 1.96	55.97 ± 1.77
	HC	45.44 ± 3.14	34.81 ± 2.34	48.47 ± 2.12	49.84 ± 1.31	64.14 ± 2.41	63.96 ± 2.61

Note: Here, 'ALL' means the combination of five EEG frequency band wavelet packet features.

Table 8
Average classification accuracies (±standard deviation) of nonlinear dynamic feature across different frequency bands using SVM with RBF kernel.

Nonlinear dynamic feature	Group	Emotional EEG frequency band					
		Delta (%)	Theta (%)	Alpha (%)	Beta (%)	Gamma (%)	ALL (%)
ApEn	PD	40.58 ± 2.06	41.99 ± 2.20	47.75 ± 2.40	65.60 ± 1.91	64.68 ± 1.62	67.61 ± 1.36
	HC	42.04 ± 2.16	45.39 ± 1.89	48.36 ± 1.62	72.01 ± 1.56	67.94 ± 1.54	73.17 ± 1.57
HE	PD	40.72 ± 1.79	40.19 ± 2.13	52.84 ± 2.02	61.50 ± 1.32	60.76 ± 2.00	65.05 ± 1.99
	HC	44.68 ± 2.06	45.55 ± 1.30	58.50 ± 1.64	67.63 ± 2.06	67.05 ± 1.90	69.34 ± 2.01
DFA	PD	38.73 ± 2.29	38.89 ± 3.20	43.75 ± 2.57	62.59 ± 2.52	61.53 ± 1.45	66.93 ± 1.95
	HC	41.34 ± 1.53	38.66 ± 2.41	48.10 ± 1.86	68.17 ± 1.93	67.61 ± 1.74	73.12 ± 1.73

Note: Here, 'ALL' means the combination of five EEG frequency band nonlinear features.

The classification performance of the PCA method is shown in Fig. 5(a). The horizontal axis denotes the number of principal components used for classification, and the vertical axis denotes the average classification accuracy. It can be noted that when the feature dimension reaches a certain number (30 principal components), the average classification accuracy becomes almost stable. This number is much smaller than the dimension of the original features. However, there exist differences in classification performance between PD patients and HC. Fig. 5(b) illustrates the average classification accuracy of using the ICA approach. Again, when the feature dimension reaches a certain number, the average classification accuracy becomes almost stable. Obviously this number is smaller than the dimension of the original features. The classification performance of the CFS approach is shown in Fig. 5(c). When the dimension of feature reaches about 40, the average classification accuracy becomes almost stable, and the average accuracy is about 72.60% ± 2.48% and 78.89% ± 2.79% for PD patients and HC, respectively. Obviously this number is smaller than the dimension of the original features.

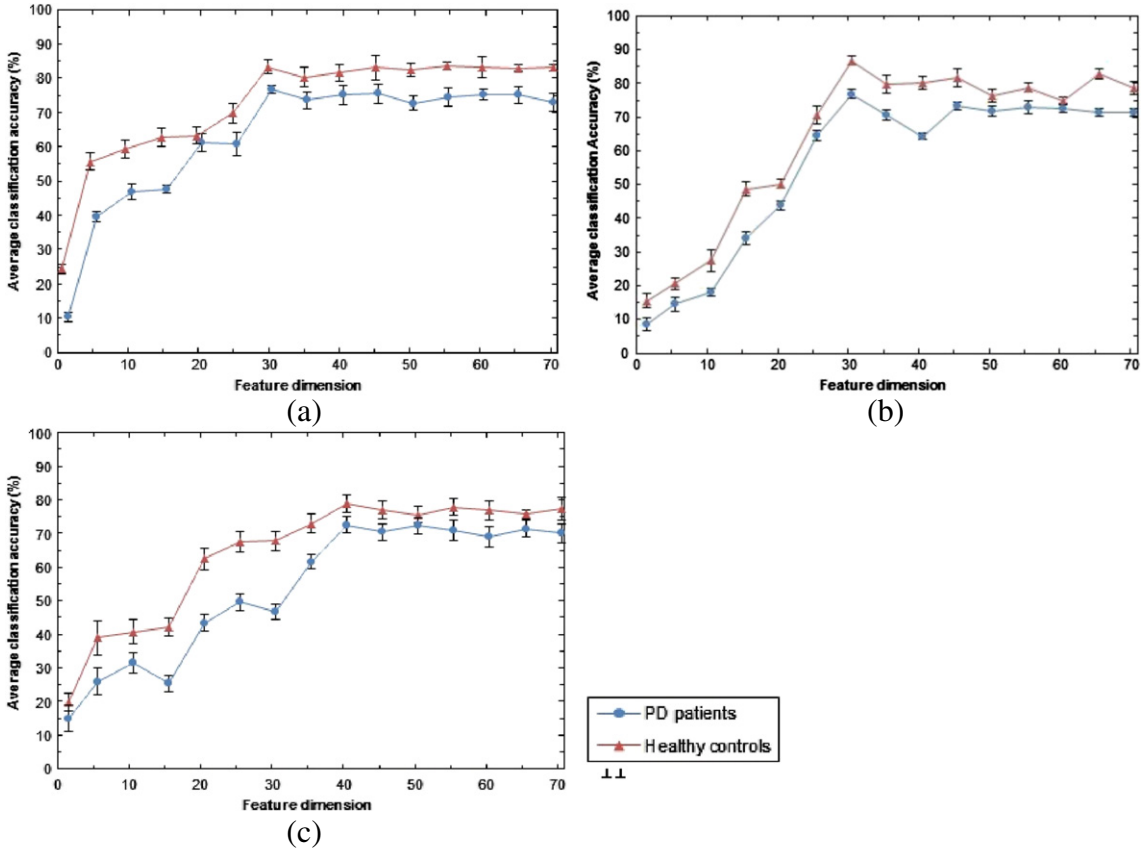

Fig. 5. Comparison of feature dimensionality reduction methods across ALL frequency bands (a) the process of PCA (b) the process of ICA (c) the process of CFS.

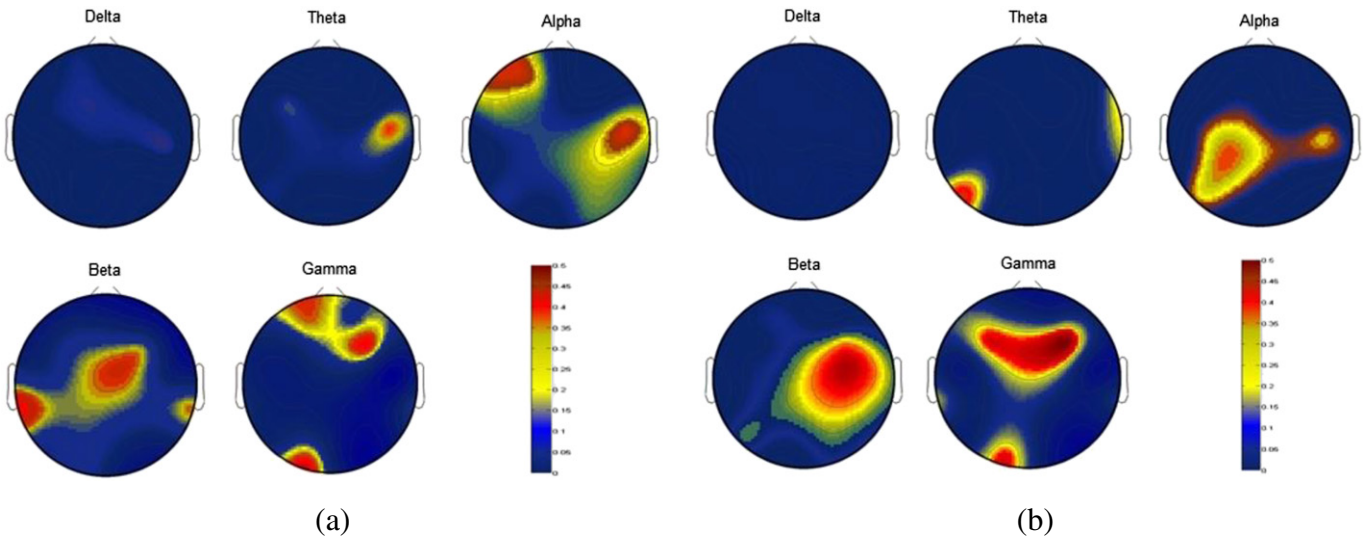

Fig. 6. Distribution of top 40 subject-independent features (a) PD patients (b) healthy controls.

From Fig. 5(a)–(c), it can be noted that the best average classification accuracy of 76.90% ± 1.48 and 86.78% ± 1.34% is obtained for PD patients and HC, respectively using ICA method when the number of feature dimensions is reduced to 30, whereas the average performance of using PCA is slightly better (76.78% ± 1.08 and 83.30 ± 2.08 for PD patients and HC, respectively) and appears to be more stable. The merit of PCA is that the extracted components have minimum correlation along the principal axes, but PCA cannot be used to find the emotion-specific features since the data is transformed to the PCA domain. In contrast, the features selected by CFS were directly computed from features. Therefore, the discriminative emotion-related brain areas and frequency bands could be found by CFS.

The distribution of top 40 subject-independent features in PD patients and healthy controls (since the classification accuracies of CFS method become almost stable after the dimension reaches about 40) is shown in Fig. 6. As can be seen, none of the top 40 features are in the delta band and very few are in the theta band. This may suggest that the delta and theta bands have little relationship with emotion. This result contrasts with previous findings of EEG–emotion correlation in these bands (Aftanas and Golocheikine, 2001; Sammler et al., 2007) since the approaches to data analysis varied from study to study. In PD patients, the selected subject-independent features were mainly in the left frontal lobe and temporal lobe for the alpha band, the temporal lobe beta band, and right occipital lobe and anterior frontal lobe for gamma band. Whereas, in HC, the selected subject-independent features were in the left parietal lobe for the alpha band, the right temporal and parietal lobe for the beta band, and the left occipital and frontal lobes for the gamma band. The emotion-related brain areas finding in HC is nearly consistent with the emotion studies of other researchers (Davidson et al., 1985; Guntekin and Basar, 2007; Schutter et al., 2001), however, none of the studies investigated PD patients.

5.6 . Trajectory of emotion changes

In order to find the trajectory of emotion changes in PD patients and HC during the experiment, we place the selected top 40 subject-independent features into the manifold model and reduced the features into one dimension using the Isomap method. The trajectory of emotion changes is as shown in Fig. 7. The horizontal axis denotes the time, and the vertical axis denotes the emotional value estimated by Isomap. The dashed red line represents the emotional state labels (i.e. reference) where positive emotions (happiness, surprise) are labeled as +1 and negative emotions (sadness, fear, disgust, anger) are labeled as −1. The solid blue line indicates the values Isomap estimation. During the experiment, emotional stimuli were presented at random order. It can be seen that the changes of the trajectory obtained by Isomap are

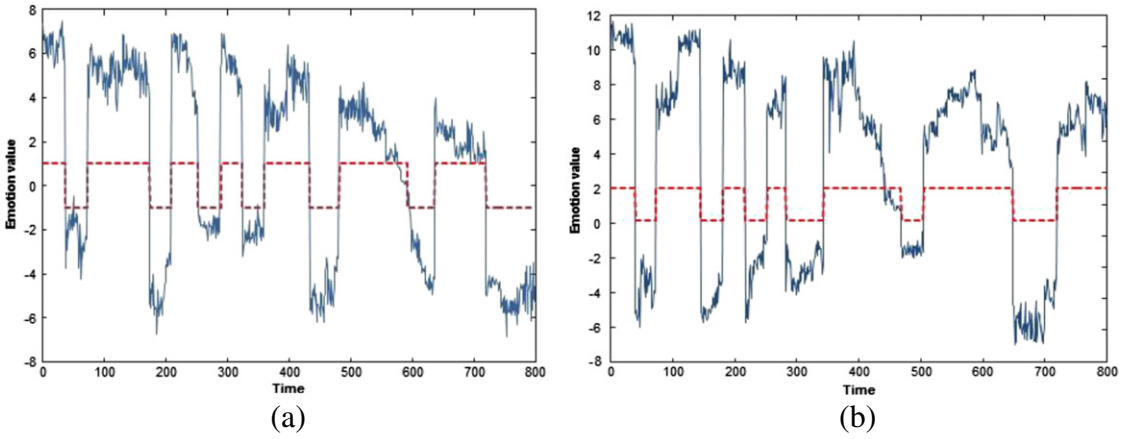

Fig. 7. The trajectory of emotion changes of (a) 20 PD patients and (b) 20 healthy controls during the experiment.

consistent with the change of emotional states. We can also observe that the estimated emotional values decrease from HC participant to PD patients during the evoking of the emotions. This is due to the dynamic processes underlying the EEG recording that are less complex for PD patients than HC during emotion processing.

6 . Conclusion

Non-motor symptoms, including disruptions in emotion information processing have been found in over 50% of newly diagnosed PD patients. In this study, we investigated the characteristics of EEG features of PD patients in comparison with HC for emotion classification and a technique for tracking the trajectory of emotion changes. Multimodal stimulus was designed to arouse six emotional states (happiness, sadness, fear, anger, surprise, and disgust) of the participants and EEG data from 20 PD patients and 20 HC were recorded. Four kinds of features, namely bispectrum, power spectrum, wavelet packet, and nonlinear dynamical analysis were extracted to assess the association between the EEG data and emotional states. Experimental results demonstrate that bispectrum across ALL frequency bands was the most robust feature among all four kinds of features discussed above, and higher frequency bands play more important role in emotion activities than lower frequency bands in both groups. However, the use of small number of PD samples affects the reliability of the system. In order to generalize the proposed algorithm, further studies should use larger number of samples to examine the relationship between brain activity and emotions in PD.

Furthermore, three feature dimensionality reduction methods, namely PCA, ICA, and CFS were implemented on the feature set. The best average classification accuracy of 76.90% ± 1.08% and 86.78% ± 2.08% for PD patients and HC was achieved by using ICA method when the number of feature dimension was reduced to 30. The top 40 subject-independent features most relevant to emotion were selected by the CFS method. Through these subject-independent features, we found the emotion-related brain areas in PD patients and HC. The trajectory of emotion changes was obtained by a manifold learning model. This provided a promising way of implementing visualization of patient's emotional state in real time and could lead to a practical system for noninvasive assessment of the emotional impairments associated with neurological disorders. The future development of this research will be focused on analyzing each of the six emotional state differences of PD patients compared with HC.

Acknowledgments

The research was financially supported by the Ministry of Science and Technology (MOSTI), Malaysia. Grant Number: 9005-00053. The authors would like to thank Dr. Mohamad Fadli, Dr. Siva Rao Subramanian and Dr. Shahrul Azmin for their assistance with recruitment of PD participants. Also we would like to thank all the individuals who participated in this study.

Appendix

[1]The following pictures in the database were used for emotion induction: *Disgust*: 1945, 2352.2, 3000, 3010, 3015, 3030, 3051, 3060, 3061, 3071, 3080, 3110, 3120, 3130, 3140, 3150,3160, 3250, 3400, 7360, 7361, 7380, 8230, 9040, 9042, 9181, 9290, 9300, 9320, 9330, 9373, 9390, 9405, 9490, 9570, and 9830; *Fear*: 1019, 1022, 1030, 1040, 1050, 1051, 1052, 1070, 1080, 1090, 1110, 1111, 1113, 1120, 1200, 1201, 1220, 1230, 1240, 1280, 1274, 1300, 1301, 1302, 1321, 1390, 1930, 1931, 3280, 5970, 5971, 5972, 6370, 9584, 9594, and 9592; *Sadness*: 2205, 2271, 2276, 2490, 2520, 2590, 2700, 2800, 2900, 3220, 3230, 3300, 3301, 3350, 6570, 6838, 8010, 9000, 9041, 9050, 9120, 9190, 9210, 9220, 9331, 9410, 9415, 9470, 9520, 9530, 9561,9611, 9910, 9911, 9920, and 9921.

[2]The following sounds in the database were used for emotion induction: *Disgust*: 134, 115, 251, 262, 284, 698, 702, 711, 712, 713, 714, 720, 728, 729, 730, 732, 812, and 813; *Fear*: 106, 133, 170, 171, 275, 276, 277, 279, 291, 312, 378, 380, 424, 425, 500, 626, 627, 699, and 817; *Sadness*: 115, 150, 260, 261, 278, 280, 285, 286,290, 293, 295, 310, 311, 368, 403, 420, 422, 501, 600, and 625.

References

Adolphs, R., Damasio, H., Tranel, D., Damasio, A.R., 1996. Cortical systems for the recognition of emotion in facial expressions. J. Neurosci. 16, 7678–7687.
Adolphs, R., Schul, R., Tranel, D., 1998. Intact recognition of facial emotion in Parkinson's disease. Neuropsychology 12, 253–258.
Aftanas, L.I., Golocheikine, S.A., 2001. Human anterior and frontal midline theta and lower alpha reflect emotionally positive state and internalized attention: high resolution EEG investigation of meditation. Neurosci. Lett. 310, 57–60.
Aftanas, L.I., Reva, N.V., Varlamov, A.A., Pavlov, S.V., Makhnev, V.P., 2004. Analysis of evoked EEG synchronization and desynchronization in emotional activation in humans: temporal and topographic characteristics. Neurosci. Behav. Physiol. 34, 859–867.
Aftanas, L.I., Reva, N.V., Savotina, L.N., Makhnev, V.P., 2006. Neurophysiological correlates of induced discrete emotions in humans: an individually oriented analysis. Neurosci. Behav. Physiol. 36, 119–130.
Aftanasa, L.I., Lotovaa, N.V., Koshkarova, V.I., Pokrovskajaa, V.L., Popova, S.A., Makhneva, V.P. , 1997. Non-linear analysis of emotion EEG: calculation of Kolmogorov entropy and the principal Lyapunov exponent. Neurosci. Lett. 226, 13–16.
Anderson, K., McOwan, P.W., 2006. A real-time automated system for the recognition of human facial expressions. IEEE Trans. Syst. Man Cybern. B 36, 96–105.
Ariatti, A., Benuzzi, F., Nichelli, P., 2008. Recognition of emotions from visual and prosodic cues in Parkinson's disease. Neurol. Sci. 29, 219–227.
Balasubramanian, M., Schwartz, E., 2002. The isomap algorithm and topological stability. Science 295, 7.
Balconi, M., Lucchiari, C., 2008. Consciousness and arousal effects on emotional face processing as revealed by brain oscillations. A gamma band analysis. Int. J. Psychophysiol. 67, 41–46.
Baumgartner, T., Esslen, M., Jancke, L., 2006. From emotion perception to emotion experience: emotions evoked by pictures and classical music. Int. J. Psychophysiol. 60, 34–43.
Beck, A.T., Ward, C.H., Mendelson, M., Mock, J., Erbaugh, J., 1961. An inventory for measuring depression. Arch. Gen. Psychiatry 4, 561–571.
Bradley, M.M., Lang, P.J., 2007. International affective digitized sounds (2nd Edition; IADS-2): affective ratings of sounds and instruction manual. Technical Report B-3 University of Florida, Gainesville, FL.
Caekebeke, J.F., Jennekens-Schinkel, A., VanderLinden, M.E., Buruma, O.J., Roos, R.A., 1991. The interpretation of dysprosody in patients with Parkinson's disease. J. Neurol. Neurosurg. Psychiatry 54, 145–148.
Chanel, G., Kierkels, J.J.M., Soleymani, M., Pun, T., 2009. Short-term emotion assessment in a recall paradigm. Int. J. Hum. Comput. Stud. 67, 607–627.
Chang, C., Lin, C., 2001. A library for support vector machines. (Available at) http://www.csie.ntu.edu.tw/~cjlin/libsvm/.
Clark, U.S., Neargarder, S., Cronin-Golomb, A., 2008. Specific impairments in the recognition of emotional facial expressions in Parkinson's disease. Neuropsychologia 46, 2300–2309.
Dara, C., Monetta, L., Pell, M.D., 2008. Vocal emotion processing in Parkinson's disease: reduced sensitivity to negative emotions. Brain Res. 1188, 100–111.
Davidson, R.J., 2004. What does the prefrontal cortex "do" in affect: perspectives on frontal EEG asymmetry research. Biol. Psychol. 67, 219–233.
Davidson, R.J., Schaffer, C.E., Saron, C., 1985. Effects of lateralized presentations of faces on self-reports of emotion and EEG asymmetry in depressed and non-depressed subjects. Psychophysiology 22, 353–364.
Dujardin, K., Blairy, S., Defebvre, L., Duhem, S., Noël, Y., Hess, U., Destée, A., 2004. Deficits in decoding emotional facial expressions in Parkinson's disease. Neuropsychologia 42, 239–250.
Fahn, S., Elton, R.L., Committee, M., 1987. Unified Parkinson's Disease Rating Scale. In: Fahn's, Marsden, C.D., Calne, D.B., Goldstein, M., Clane, D.B. (Eds.), Recent Developments in Parkinson's Disease2. Macmillan Health Care Information, Florham Park, pp. 153–163.
Folstein, M.F., Folstein, S.E., Mchugh, P.R., 1975. Mini-Mental State Examination: a practical method for grading the cognitive state of patients. Psychol. Res. 12, 189–198.
Gotlib, I.H., Raganathan, C., Rosenfeld, J.P., 1998. Frontal EEG alpha asymmetry, depression, and cognitive functioning. Cogn. Emot. 12, 449–478.
Gray, H.M., Tickle-Degnen, L., 2010. A meta-analysis of performance on emotion recognition tasks in Parkinson's disease. Neuropsychology 24, 176–191.
Gunes, H., Piccardi, M., 2007. Bi-modal emotion recognition from expressive face and body gestures. J. Netw. Comput. Appl. 30, 1334–1345.
Guntekin, B., Basar, E., 2007. Emotional face expressions are differentiated with brain oscillations. Int. J. Psychophysiol. 64, 91–100.
Hadjidimitriou, S.K., Hadjileontiadis, L.J., 2012. Toward an EEG-based recognition of music liking using time–frequency analysis. IEEE Trans. Biomed. Eng. 59, 3498–3510.
Hamdi, H., Richard, P., Suteau, A., Allain, P., 2012. Emotion assessment for affective computing based on physiological responses. IEEE proc. World Congress on Computational Intelligence (WCCI), pp. 10–15.
Hoehn, M.M., Yahr, M.D., 1967. Parkinsonism: onset, progression and mortality. Neurology 17, 427–442.

Hyvarinen, A., Oja, E., 2000. Independent component analysis: algorithms and applications. Neural Netw. 13, 411–430.
Jeong, J., Kim, S.Y., Han, S.H., 1998. Non-linear dynamical analysis of the EEG in Alzheimer's disease with optimal embedding dimension. Electroencephalogr. Clin. Neurophysiol. 106, 220–228.
Kan, Y., Kawamura, M., Hasegawa, Y., Mochizuki, S., Nakamura, K., 2002. Recognition of emotion from facial, prosodic and written verbal stimuli in Parkinson's disease. Cortex 38, 623–630.
Kessous, L., Castellano, G., Caridakis, G., 2010. Multimodal emotion recognition in speech-based interaction using facial expression, body gesture and acoustic analysis. J. Multimodal User Interfaces 3, 33–48.
Kober, H., Barrett, L.F., Joseph, J., Bliss-Moreau, E., Lindquist, K., Wagera, T.D., 2008. Functional grouping and cortical–subcortical interactions in emotion: a meta-analysis of neuroimaging studies. Neuroimage 42, 998–1031.
Lang, P.J., Bradley, M.M., Cuthbert, B.N., 2008. International affective picture system (IAPS): affective ratings of pictures and instruction manual. Technical Report A-8. University of Florida, Gainesville, FL.
Lawrence, A.D., Goerendt, I.K., Brooks, D.J., 2007. Impaired recognition of facial expression of anger in Parkinson's disease patients acutely withdrawn from dopamine replacement therapy. Neuropsychologia 45, 65–74.
Lima, C.F., Garrett, C., Castro, S.L., 2013. Not all the sounds sound the same: Parkinson's disease affects differently emotion processing in music and in speech prosody. J. Clin. Exp. Neuropsychol. 35, 373–392.
Lin, Y.P., Wang, C.H., Wu, T.L., Jeng, S.K., Duann, J.R., Chen, J.H., 2010. EEG-based emotion recognition in music listening. IEEE Trans. Biomed. Eng. 57, 1798–1806.
Martinez-Martin, P., Blazquez, C.R., Kurtis, M.M., Chaudhuri, K.R., 2011. The impact of non-motor symptoms on health-related quality of life of patients with Parkinson's disease. Mov. Disord. 26, 399–406.
Mikels, J., Fredrickson, B., Larkin, G., Lindberg, C., Maglio, S., Reuter-Lorenz, P., 2005. Emotional category data on images from the international affective picture system. Behav. Res. Methods 37, 630–636.
Murugappan, M., Nagarajan, R., Yaacob, S., 2010. Combining spatial filtering and wavelet transform for classifying human emotions using EEG signals. J. Med. Biol. Eng. 31, 45–51.
Nikias, C.L., Petropulu, A., 1993. Higher-order Spectral Analysis: a Nonlinear Signal Processing Framework. Prentice Hall, Englewood Cliffs, NJ.
Oathes, D.J., Ray, W.J., 2008. Worry, generalized anxiety disorder, and emotion: evidence from the EEG gamma band. Biol. Psychol. 79, 165–170.
Oldfield, R.C., 1971. The assessment and analysis of handedness: the Edinburgh Inventory. Neuropsychologia 9, 97–113.
Park, H., 2012. ISOMAP induced manifold embedding and its application to Alzheimer's disease and mild cognitive impairment. Neurosci. Lett. 513, 141–145.
Pell, M.D., Leonard, C.L., 2003. Processing emotional tone from speech in Parkinson's disease: a role for the basal ganglia. Cogn. Affect. Behav. Neurosci. 3, 275–288.
Pell, M.D., Leonard, C.L., 2005. Facial expression decoding in early Parkinson's disease. Cogn. Brain Res. 23, 327–340.
Peron, J., Biseul, I., Leray, E., 2010. Subthalamic nucleus stimulation affects fear and sadness recognition in Parkinson's disease. Neuropsychology 24, 1–8.
Péron, J., Dondaine, T., Jeune, F.L., Grandjean, D., Vérin, M., 2012. Emotional processing in Parkinson's disease: a systematic review. Mov. Disord. 27, 186–199.
Petrantonakis, P.C., Hadjileontiadis, L.J., 2010. Emotion recogntion from brain signals using hybrid adaptive filtering and higher order crossings analysis. IEEE Trans. Affect. Comput. 1, 81–96.
Petrantonakis, P.C., Hadjileontiadis, L.J., 2011. A novel emotion elicitation index using frontal brain asymmetry for enhanced EEG-based emotion. IEEE Trans. Inf. Technol. Biomed. 15, 737–746.
Pincus, S., 1995. Approximate entropy (apen) as complexity measure. Chaos 5, 110–117.
Pincus, S.M., Goldberger, A.L., 1994. Physiological time-series analysis: what does regularity quantify? Am. J. Physiol. 266 (4 Pt 2), H1643–H1656.
Redondo, J., Fraga, I., Padron, I., Pineiro, A., 2008. Affective ratings of sound stimuli. Behav. Res. Methods 40, 784–790.
Sammler, D., Grigutsch, M., Fritz, T., Koelsch, S., 2007. Music and emotion: electrophysiological correlates of the processing of pleasant and unpleasant music. Psychophysiology 44, 293–304.
Schmidt, L.A., Trainor, L.J., 2001. Frontal brain electrical activity (EEG) distinguishes valence and intensity of musical emotions. Cogn. Emot. 15, 487–500.
Schröder, C., Möbes, J., Schütze, M., Szymanowski, F., Nager, W., Bangert, M., Münte, T.F., Dengler, R., 2006. Perception of emotional speech in Parkinson's disease. Mov. Disord. 21, 1774–1778.
Schutter, D.J.L., Putman, P., Hermans, E., vanHonk, J., 2001. Parietal electroencephalogram beta asymmetry and selective attention to angry facial expressions in healthy human subjects. Neurosci. Lett. 314, 13–16.
Tenenbaum, J.B., deSilva, V., Langford, J.C., 2000. A global geometric framework for nonlinear dimensionality reduction. Science 290, 2319–2323.
Valenza, G., Lanata, A., Scilingo, E.P., 2012. The role of nonlinear dynamics in affective valence and arousal recognition. IEEE Trans. Affect. Comput. 3, 237–249.
Wang, Y., Guan, L., 2008. Recognizing human emotional state from audiovisual signals. IEEE Trans. Multimed. 10, 659–668.
Wang, X.W., Nie, D., Lu, B.L., 2013. Emotional state classification from EEG data using machine learning approach. Neurocomput. 129, 94–106.
Wieser, M.J., Klupp, E., Weyers, P., Pauli, P., Weise, D., Zeller, D., Classen, J., Muhlberger, A., 2012. Reduced early visual emotion discrimination as an index of diminished emotion processing in Parkinson's disease?—Evidence from event-related brain potentials. Cortex 48, 1207–1217.
Yip, J.T., Lee, T.M., Ho, S.L., Tsang, K.L., Li, L.S., 2003. Emotion recognition in patients with idiopathic Parkinson's disease. Mov. Disord. 18, 1115–1122.
Yuvaraj, R., Murugappan, M., Norlinah, M.I., Iqbal, M., Sundaraj, K., Mohamad, K., Palaniappan, R., Satiyan, M., 2014. Emotion classification in Parkinson's disease by higher-order spectra and power spectrum features using EEG signals: a comparative study. J. Integr. Neurosci. 13, 1–32.
Zhang, Q., Lee, M., 2009. Analysis of positive and negative emotions in natural scene using brain activity and GIST. Neurocomput. 72, 1302–1306.